Journal of Marine Science and Technology

Volume 31 | Issue 1 Article 4

Exhaust Noise Elimination Using Silencers Fortified with Perforated Tubes, Extended Tubes, Penetrable Resin Inlet and Orifice Plate

Min-Chie Chiu
Department of Mechanical and Materials Engineering, Tatung University, ROC, minchie.chiu@msa.hinet.net

Ho-Chih Cheng
Department of Information Technology, Ling Tung University, Taiwan, ROC

DOI: 10.51400/2709-6998.2683
Available at: https://jmstt.ntou.edu.tw/journal/vol31/iss1/4

RESEARCH ARTICLE

Exhaust Noise Elimination Using Silencers Fortified With Perforated Tubes, Extended Tubes, Penetrable Resin Inlet and Orifice Plate

Min-Chie Chiu [a,*], Ho-Chih Cheng [b]

[a] Department of Mechanical and Materials Engineering, Tatung University, Taiwan, ROC
[b] Department of Information Technology, Ling Tung University, Taiwan, ROC

Abstract

Pneumatic equipment in marine diesel engine and associated piping system often emit extremely high level of noises when releasing pressure. Concerning the crew's hearing health, discovering an efficient noise silencing device becomes essential.

A silencer fortified with extended tubes, perforated tubes, orifice plate, and penetrable resin inlet is presented in order to competently dampen the blown-up noises. A simplified objective function by means of FEM, Artificial Neural Networks (ANNs), and a Genetic Algorithm (GA) is established to enable the numerical calculation when using a finite element method.

Three silencer designs, silencer A (with element A, a penetrable resin inlet), B (with element B, a shell composing of extended tubes, perforated tubes and orifice plate), and C (combined with element A and element B), are proposed in this study. The sound transmission of these silencers is analyzed using a finite element program (COMSOL). Additionally, silencer C is numerically optimized using FEM together with Artificial Neural Network and Genetic Algorithm. In order to investigate the efficiency of silencer's noise abatement, three frequencies (500 Hz, 3000 Hz, and 5000 Hz) representing the whole frequency region are selected as the target frequencies during the Transmission Loss (TL) optimization.

Consequently, the shape-optimized silencers within a space-constrained situation are easily accomplished.

Keywords: Exhaust, Genetic algorithm, Neural network, Optimization, Penetrable, Orifice

1. Introduction

Delany and Bazley [1] started the derivation of sound absorbing ability for porous material in 1969. The related flow resistance from the bulk density of the material was proposed. Johnson [2] estimated sound absorbing ability via four parameters. Later, Champoux and Allard [3] established thermal characteristics length as an acoustical parameter in 1991. Lafarge et al. [4] also used a Johnson-Champoux-Allard model in evaluating sound absorbing ability by means of five acoustical parameters. In this theory, an assumption of equivalent flow property of the acoustical material is made in advance. Sound absorbing materials have been used in muffler designs. Cummings [5] analyzed the TL on a curve channel which was inserted with both rectangular and circular acoustical splitters. Rostafinski [6], in 1974, proposed a formula of sound propagation within a curve channel. Fuller and Bies [7] undertook an experimental study of the TL by varying channel shapes (both the straight channel and curve channel) and cross-sections in 1978. Selamet et al. [8], in 1994, published a transmission loss's prediction for a Hershel-Quinckee tube by means of both theoretical method and experimental measurement. Kim and Ih [9] estimated TL in a bent extension chamber via a four-pole matrix in 1999. Results revealed that the TL curve was narrowed at a specified frequency region.

Received 6 December 2022; revised 1 January 2023; accepted 4 January 2023.
Available online 31 March 2023

* Corresponding author at: Department of Mechanical and Materials Engineering, Tatung University, No. 40, Sec. 3, Zhongshan N. Rd., Taipei, 10452, Taiwan, ROC.
E-mail address: minchie.chiu@msa.hinet.net (M.-C. Chiu).

https://doi.org/10.51400/2709-6998.2683

The research works mentioned above were aimed to solve the engineering problem of noise. In real world, impulse noises occur on land in factories [10] and at sea in ships. As a noise problem on board of a ship, loud noises are emitted from the piping system of a marine diesel engine [11,12]. For the crew's hearing health, a noise abatement of marine diesel engine's venting noise using silencers is obligatory [13,14]. A plug device with pores has been habitually installed on the venting outlet of the pneumatic equipment such as diesel engine and its pipe system. However, the TL of the penetrable plug was not sufficient in depressing the noise energy. Therefore, a new acoustical element added to the porous plug is obligatory to reduce the noise level. Here, three silencers (Silencer A: with penetrable resin inlet (element A); Silencer B: with a shell having extend tubes, perforated tubes and orifice plate (element B); and Silencer C: element A (penetrable resin inlet) + element B (a shell having extended tubes, perforated tubes and orifice plate) are introduced.

FEM (Finite Element Method) has been implemented in acoustical simulation in, for example, dealing with mufflers with complicated acoustical mechanism. Dhaiban et al. analyzed elliptical muffler chambers using FEM [15]. Fu et al. improved muffler structure using acoustic FEM analysis [16]. However, it is complicated and takes a long time in computer calculation throughout the shape optimization [17]. To shorten the process, Chiu and Chang et al. [18] developed a simplified mathematical formula by means of Artificial Neural Network (ANN) along with optimizer. Therefore, a simplified mathematical model via Artificial Neural Network (ANN) together with GA optimizer is adopted in the silencer optimization. In this study, three silencers (silencer AC) are analyzed using a FEM software, and simplified mathematical formula introduced in silencer C's optimization. For the optimization, three target frequencies (500 Hz, 3000 Hz, and 5000 Hz) are nominated during the optimization.

2. Mathematical formula of the FEM (on COMSOL)

The three silencer designs proposed (Silencer A: with element A (penetrable resin inlet); Silencer B: with element B (a shell with extended tubes, perforated tubes and orifice plate); and Silencer C: element A (penetrable resin inlet) + element B (a shell with extended tubes, perforated tubes, and orifice plate)) are presented in Fig. 1. The solid boundary's acoustical boundary condition in the COMSOL software is

$$n\cdot\left\{\frac{1}{\rho_c}\left(\nabla p_t - q_d\right)\right\}=0 \tag{1}$$

where

$$p_t = p + p_b$$

p_t is the sum of a possible background pressure p_b and the scattered pressure p.

q_d (a dipole sound source) is preset at zero, c (a sound speed) is preset at 343 (m/s), and ρ_c (an air density) is preset at 1.293 (kg/m^3).

Nomenclature

The following symbols are used herein for the purpose of this paper:

Bit_n	bit length of chromosome
BB_0, BB_i, BB_{ij}, BB_{ijk}	coefficient of ANN's node function
PPF	product of penalty function
D	diameter of perforated tube (m)
d_h	the hole's diameter of the perforated tube (m)
$iter_m$	maximal iteration number of GA optimization
L	horizontal distance of perforated tube (m)
L_1	horizontal distance of extended tube (m)
mm	amount of design parameters
MMM	accuracy of parameter search
NNN	amount of training data
N_p	total probable probing number ($=2^{mm}$)
p	acoustic pressure (Pa)
p_t	the total acoustic pressure (Pa)
p_{t1}, p_{t2}	the upstream acoustic pressure and downstream acoustic pressure (Pa)
pc_n	crossover number
pm_n	mutation number
P_{max}	the maximum range of the parameter
P_{min}	the minimum range of the parameter
pop_n	amount of population
Q	the number of horizontal holes on the orifice
q_d	a dipole sound source (N/m^3)
QQ	amount of network coefficients
t_p	the thickness of the perforated tube (m)
TL	sound transmission loss (dB)
xx_i, xx_j, xx_k	input data of ANN
yy_k	output of ANN
$\widehat{yy_i}$	required data of ANN
yy_i	forecast data of ANN
Z_i	acoustic impedance ($Pa\cdot s/m^3$)
σ	perforation rate of a perforated tube
$\sigma\sigma^2$	error deviation of ANN
φ	perforation rate of porous material
$\varnothing$	perforation rate of a perforated tube
σ_0	flow impedance ($Pa\cdot s/m^2$)
α_∞	curving level
η	shearing viscosity (kg/ms)

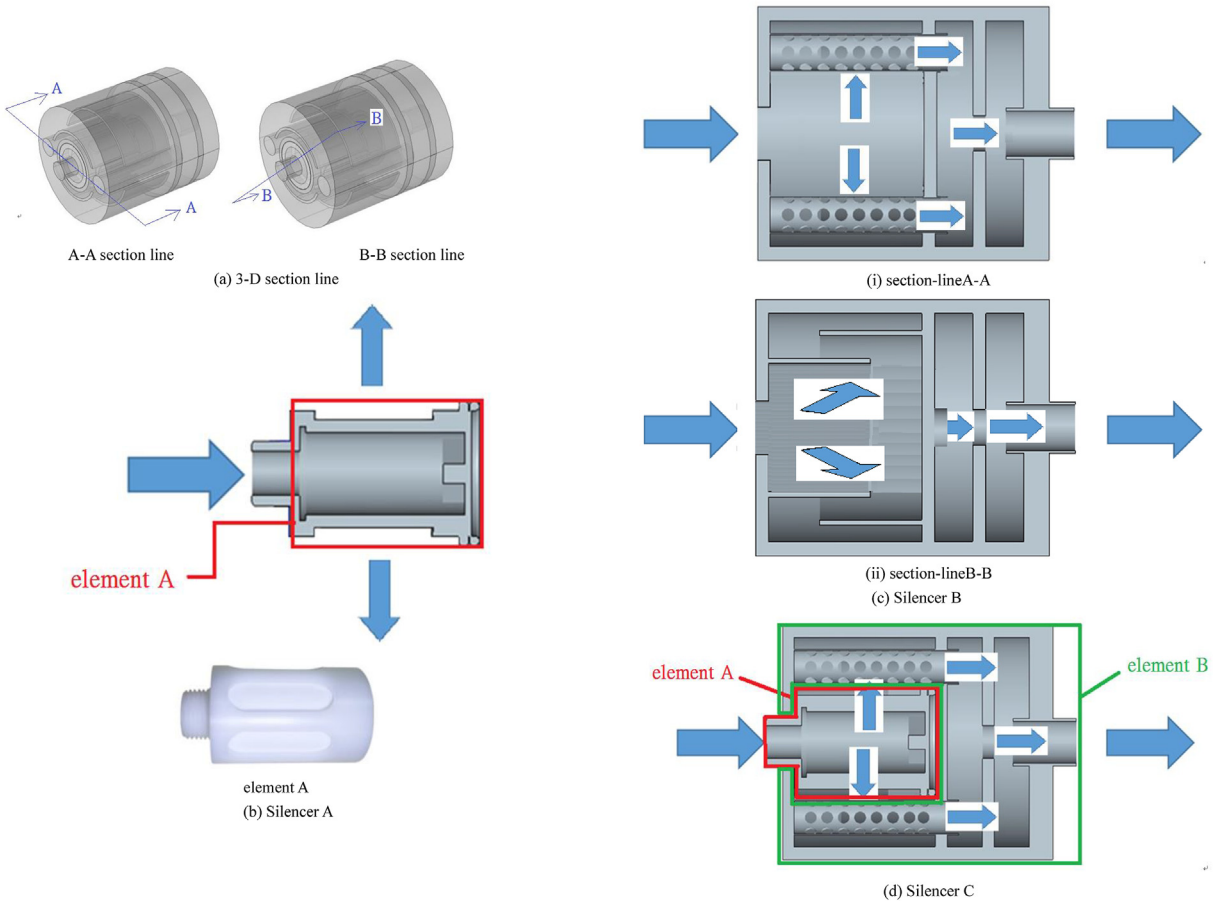

Fig. 1. Three kinds of silencers (silencer A: element A; silencer B: element B; silencer C: element A + element B).

The perforated tube's acoustical boundary condition is

$$\mathrm{n}\cdot\left\{\frac{1}{\rho}\left(\nabla p_t - q_d\right)\right\} = -\left(p_{t1} - p_{t2}\right)\frac{i\omega}{Z_i} \tag{2}$$

$$Z_i = \rho_c \cdot c_c\left[\frac{1}{\rho}\sqrt{\frac{8\mu k}{\rho_c c_c}}\left(1+\frac{t_p}{d_h}\right)+\theta_f + i\frac{k}{\sigma}\left(t_p+\delta_h\right)\right] \tag{3}$$

where ρ_c and c_c are complex-valued quantities, t_p, d_h, and σ are the thickness, the hole's diameter, and the perforation rate of the perforated tube, respectively. In addition, p_{t1} and p_{t2} represent the upstream pressure and downstream pressure, respectively.

Simulating the acoustical behavior of porous material, the Johnson-Champoux-Allard model used in COMSOL is

$$\rho_{eff} = \frac{\alpha_\infty \rho_0}{\varphi}\left(1+\frac{\sigma_0\varphi}{j\rho_0\omega\alpha_\infty}G_J(\omega)\right) \tag{4}$$

$$G_J(\omega) = \left(1+\frac{4j{\alpha_\infty}^2\eta\rho_0\omega}{{\sigma_0}^2\Lambda^2\varphi^2}\right)^{\frac{1}{2}} \tag{5}$$

where α_∞ is a curving level, η (shearing viscosity) is preset as 1.84×10^{-5} (kg/ms), and φ is the porosity of porous material. σ_0 is a flow impedance as follows

$$\sigma_0 = \frac{\mu}{\alpha} = \frac{150\mu(1-\varphi)^2}{D_p^2\varphi^3} \tag{6}$$

The bulk factor (K_{eff}) related to the curving level (α_∞) is

$$K_{eff} = \frac{\gamma P_0}{\varphi\cdot\left[\gamma-(\gamma-1)\left[1+\frac{8\eta}{j\Lambda'^2B^2\omega\rho_o}\left(1+j\rho_0\frac{\omega B^2\Lambda'^2}{16\eta}\right)^{\frac{1}{2}}\right]^{-1}\right]} \tag{7}$$

Both $\wedge$ (viscous character length) and $\wedge'$ (thermal character length) are defined as

$$\Lambda = \frac{1}{c}\left(\frac{8\alpha_\infty\eta}{\sigma_0\varphi}\right)^{\frac{1}{2}} \tag{8}$$

$$\Lambda' = \frac{1}{c'}\left(\frac{8\alpha_\infty \eta}{\sigma_0 \varphi}\right)^{\frac{1}{2}} \tag{9}$$

The propagating equation for the sound wave transmitted through the silencer yields

$$\nabla \cdot -\frac{1}{\rho_c}(\nabla p_t - q_d) - \frac{k_{eq}^2 p_t}{\rho_c} = Q \tag{10a}$$

where

$$k_{eq}^2 = \left(\frac{\omega}{c_c}\right)^2;\ c_c = c;\ \rho_c = \rho \tag{10b}$$

The acoustical performance of TL is

$$\mathrm{TL} = 10 \log \frac{W_{in}}{W_{out}} \tag{11}$$

The flow chart of silencer's acoustic simulation using the COMSOL is depicted in Fig. 2.

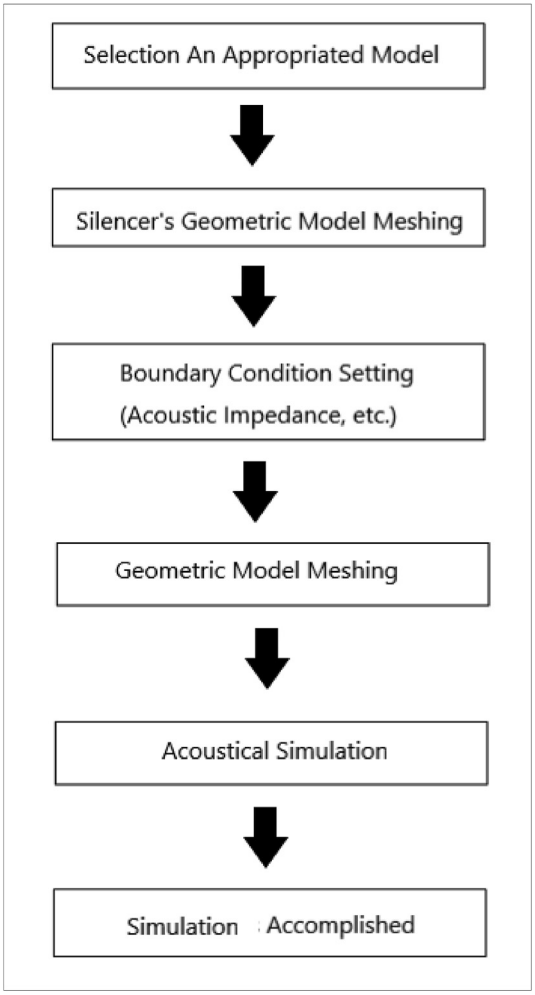

Fig. 2. The flow chart of silencer's acoustic simulation in the COMSOL.

3. Model verification

To validate the correctness of COMSOL used in silencer simulation, three silencers internally implanted with three noise abatement elements (extended tubes, perforated tubes, and penetrable resin material) are demonstrated and verified by experimental data and other theories. As indicated in Fig. 3, the TL of a one-chamber silencer muffler with internally extended and perforated tubes is calculated by COMSOL and proved by an experimental data [19]. Results divulge that they are in good agreement. Similarly, as depicted in Fig. 4, for silencer having a perforated tube, the comparison of TL curve using COMSOL simulation and experimental data [20] shows that the tendency of TL curve between the COMSOL and experimental data is mostly consistent except a little TL deviation occurring at the peak frequency. Moreover, as plotted in Fig. 5, the predicted TL of bulk wool is approximately comparable to that of the investigational data [21]. Therefore, the accuracy of simulated data using COMSOL might be acceptable. Consequently, the acoustical prediction for silencers A~C shown in Fig. 1 is performed using the COMSOL in the following section.

4. Artificial Neural Network Model

The implicit organization of ANN (Artificial Neural Network) having hidden layers is awkward when executing the calculation procedure. An explicit function expressed by a polynomial ANN is mandatory. With this in mind, the neuron interconnections within the layers can be simplified and the automatic scheme used in adjusting the weights can be built when performing a polynomial ANN [22,23]. The coefficients of polynomial ANN are acquired via a regression progression. The polynomial ANN composing of an input layer, a hidden layer, and an output layer is displayed in Fig. 6 where the j-th output (zz_{jk}) is

$$zz_{jk} = \sum_{i=0}^{n} WW_{ij} XX_{ij} \tag{12}$$

The overall output for the ANN having h's unit number of hidden layer is

$$yy_k = \prod_{j=1}^{h} z_{jk} \tag{13}$$

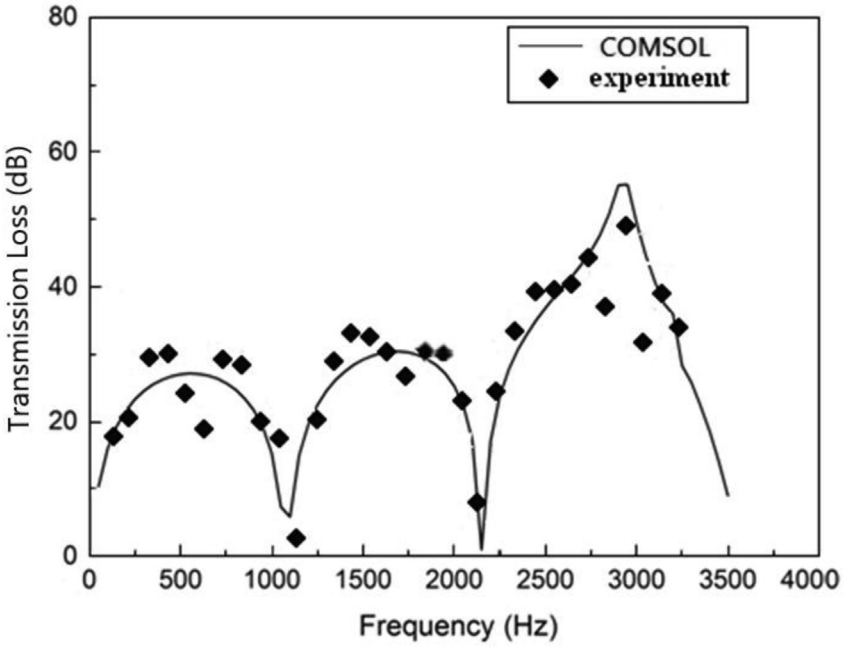

(a) comparison of TL between COMSOL and experimental data

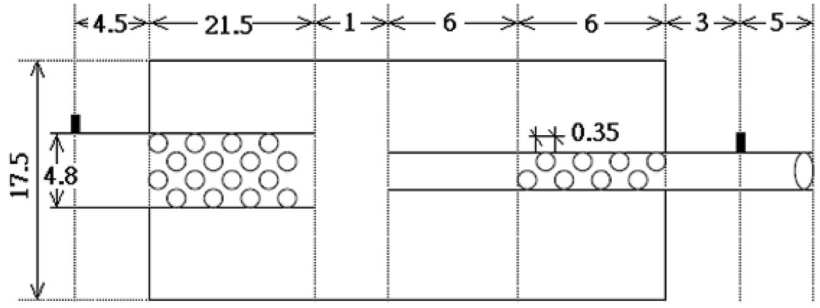

(b) muffler dimension (unit:cm) with tube's perfoated rate of φ =0.32

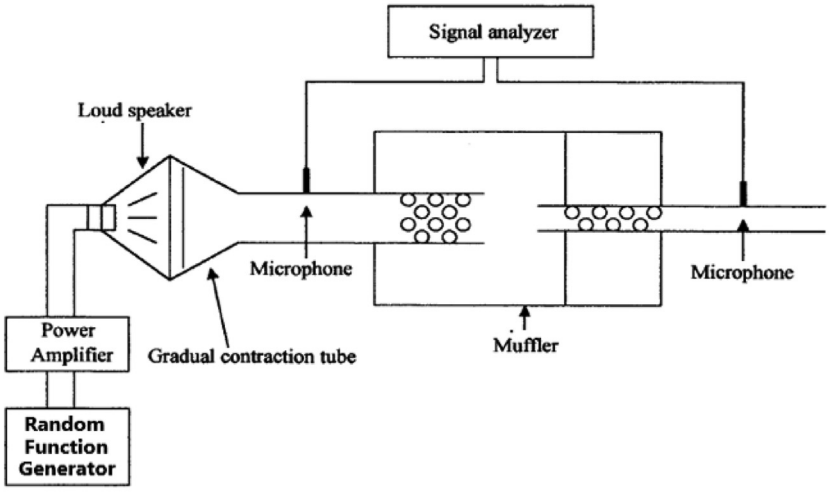

(c) experiment set-up

Fig. 3. An accuracy check of the one-chamber muffler with internally extended and perforated tubes [19].

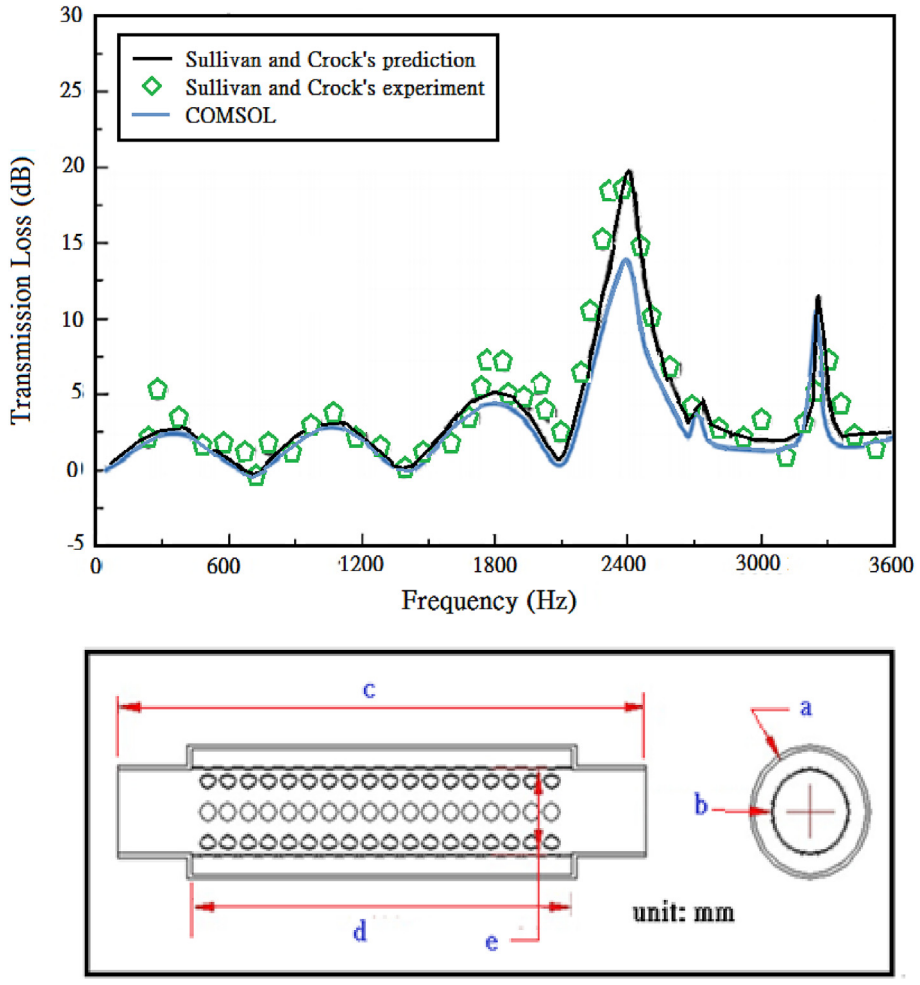

Fig. 4. Accuracy check of sound transmission loss for silencers internally inserted with a straight and perforated tube (a = 76.2; b = 52.42; c = 357.2; d = 257.2; e = 50.8) [20].

Combining with Eq. (12) and Eq. (13) yields

$$yy_k = BB_0 + \sum_{i=1}^{n} BB_{ij} xx_i + \sum_{i=1}^{n}\sum_{j=1}^{n} BB_{ij} xx_i xx_j + \sum_{i=1}^{n}\sum_{j=1}^{n}\sum_{k=1}^{n} BB_{ijk} xx_i xx_j xx_k + \cdots \quad (14)$$

where xx_i, xx_j, xx_k are the input data, yy_k is the output value, and BB_0, BB_i, BB_{ij}, and BB_{ijk} are the related node function's factors.

As illustrated in Fig. 6, silencer's design parameters and its TL (predicted by COMSOL) serve as ANN's input data and output data, respectively. An educated ANN model can be accomplished by inputting the teaching data bank and performing the polynomial scheming together with the PPSE standard. Here, PPSE (a mean square) is

$$\mathrm{PPF} = \frac{1}{NNN}\sum_{i=1}^{NNN}\left(\widehat{yy}_i - yy_i\right)\left(\widehat{yy}_i - yy_i\right)^2 + \mathrm{PPF}\frac{2\sigma\sigma^2 QQ}{NNN} \quad (15)$$

NNN, $\widehat{yy}_i$, and yy_i represent the number of teaching data, the required data, and the forecast data, respectively; PPF, $\sigma\sigma^2$, and QQ are the penalty function production, the error deviation, and the number of network factors, also respectively. The prediction of silencer's TL is achieved by substituting arbitrary silencer's geometric data into the trained ANN which serves as a simplified OBJ function. Moreover, a shape-optimized silencer is also found by using the simplified OBJ function (the educated ANN) and the Genetic Algorithm. The related simplified OBJ function, a trained ANN, is expressed as

$$\mathrm{OBJ}(\overline{X}) = BB_0 + \sum_{i=1}^{n} BB_{ij} xx_i + \sum_{i=1}^{n}\sum_{j=1}^{n} BB_{ij} xx_i xx_j + \sum_{i=1}^{n}\sum_{j=1}^{n}\sum_{k=1}^{n} BB_{ijk} xx_i xx_j xx_k + \quad (16)$$

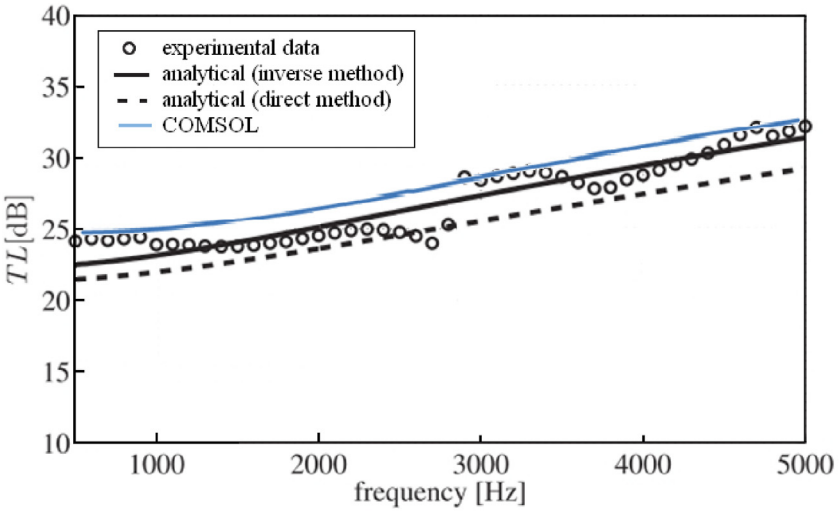

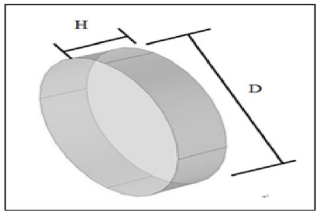

Diameter (D) [mm]	Thickness (H) [mm]	σ [Pa·s/m^2]	ϕ [–]	α_∞ [–]	Λ [μm]	Λ' [μm]
25.4	6.5	2.07E6	0.67	2.24	12.54	21.54

Fig. 5. Accuracy check of sound transmission loss for a bulk of penetrable sound absorbing material [21].

Where $\overline{X}$, including xx_i, xx_j, xx_k, is the silencer's geometric design parameter set.

5. Genetic algorithm

Genetic Algorithm (GA), one of robust algorithms, is efficiently used in pursuing global optimization [24−26]. It is proposed by Holland [27] and glowing applied in solving practical problems by Jong [28]. To achieve good optimization, five GA's controllers - pop_n (the amount of gene population), bit_n (the length of chromosome, elitism (a selection scheme), pm_n (mutation number), pc_n (crossover number), and $iter_m$ (maximal iteration in GA) - have been selected in the optimization process. Using GA controller as well as silencer's geometrical parameters, each prospective parent is selected by means of coding/decoding conversion process and the simplified OBJ. The accuracy (MMM) of parameter searching yields

$$\mathrm{MMM} = \frac{P_{max} - P_{min}}{N_p - 1} \tag{17}$$

where, N_p is in the form of 2^{mm}, mm is the total amount of the design parameters, and P_{max} and P_{min} represent the maximal and minimal ranges of the design parameter. A uniform crossover is adopted during the crossover processing. A mutation scheme is also implemented in the GA optimization process to enrich the chromosomes variety that increases gene quality, as shown in Fig. 7. Also displayed in Fig. 7, the GA optimization process is terminated when the iteration number reaches $iter_m$.

6. Sensitivity analysis

The sensitivity analysis is performed to realize the effect of TL to other design parameters. A recognition of acoustical efficiency for the silencers shown in Fig. 1 is initiated prior to the sensitivity analysis. The dimensions of the silencers are depicted in Fig. 8. The predicted TLs of silencer A ~ silencer C are plotted in Fig. 9. As displayed in Fig. 9, silencer C having both elements A and B is superior to other silencers and, therefore, chosen as the object for further sensitivity examination.

First, L (the length of perforated tube) shown in Fig. 10 is selected as the design parameter for sensitivity analysis. As depicted in Fig. 11, the L = 48 case TL spectrum is horizontally shifted to the right

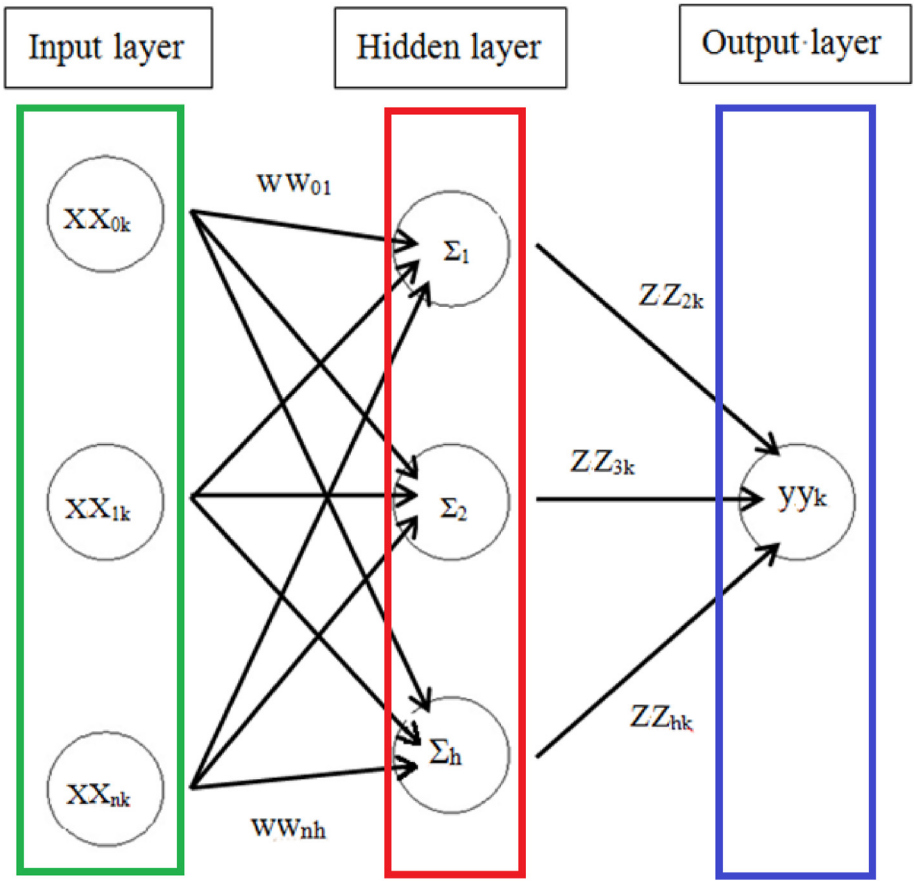

Fig. 6. The structure of a polynomial neural network.

when the frequency is below 3000, and in the case of L = 38, TL spectrum is horizontally shifted to the right when the frequency is below 2000; the change seems to vary with frequencies. However, there is no obvious tendency for the parameter L. Second, as depicted in Fig. 12, the perforated tube's perforation rate ∅ is selected for the sensitivity analysis. According to Fig. 13, the variety of TL after 2800 Hz is tuned obviously. The TL is increased with ∅ . Similarly, the length (L1) of extended tube shown in Fig. 14 is chosen as the parameter. As illustrated in Fig. 15, the TL after 1500 Hz is horizontally shifted to the right when varying the L1. Moreover, as depicted in Fig. 16, Q (number of horizontal holes on the orifice plate) is regarded as a design parameter. The result in Fig. 17 reveals that the TL after 800 Hz is obviously changed when varying the Q. For the frequency range below 2500 Hz, the TL rises as Q decreases. Likewise, the hole-allocation pattern in an orifice plate (with three holes) shown in Fig. 18 is also taken as the design parameter. There are three hole allocation, including vertically, horizontally, and uniformly allocated patterns. The estimated result in Fig. 19 reveals that the variety of TL after 1250 Hz is obvious when the pattern of hole-allocation is adjusted. For the frequency between 1250 Hz and 2300 Hz, the horizontal hole-allocation has the best effect in TL, and the uniform allocation has the worst.

7. Case study

A new type of muffler C internally inserted with element A (penetrable resin inlet) and element B (a shell with two extended tubes, two perforated tubes, and an orifice plate) is adopted to advance the acoustical efficiency for pneumatic muffler. As investigated in section 6, several geometric parameters have influences to the silencer's TL. To simplify the silencer optimization process, two geometric parameters (perforated tube's diameter

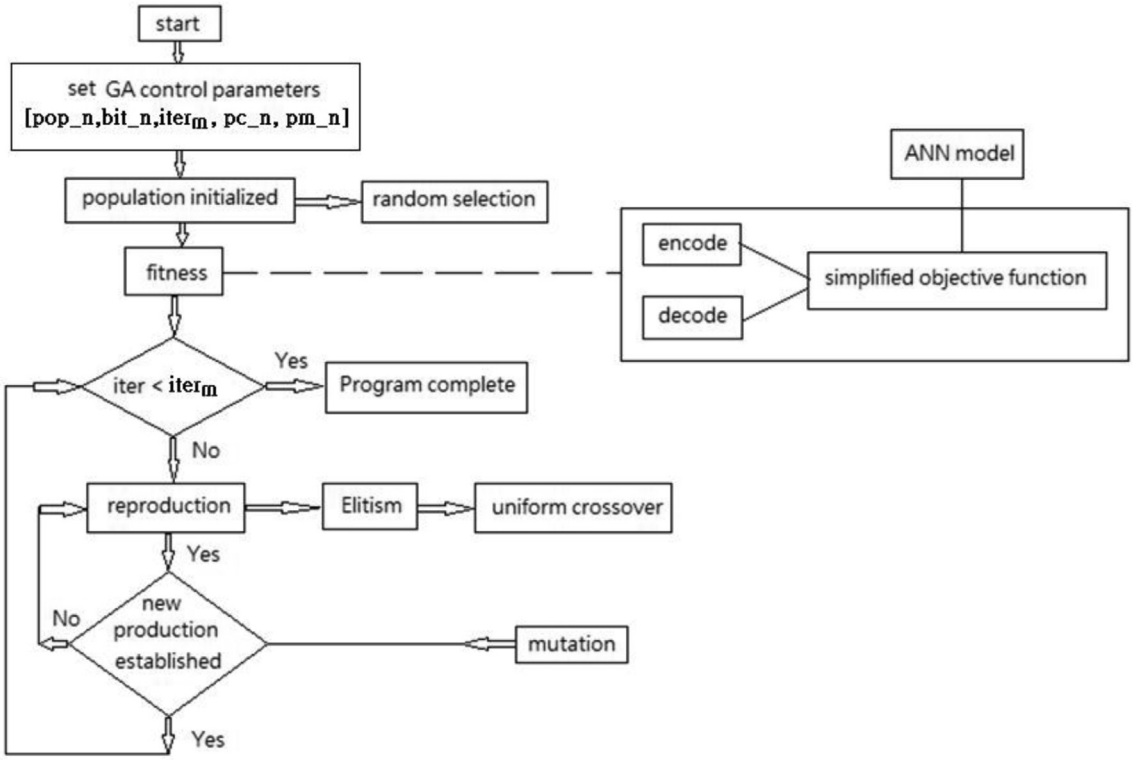

Fig. 7. Flow chart of GA optimization.

(D) and length (L)) are elected and depicted in Fig. 20.

The schedule levels and parameter range are shown in Table 1. The predicted TL using sixteen teaching data sets (as shown in Table 2) is obtained by running a COMSOL simulation for the silencer's design. In the ANN organization, both D and L are the input data, and TL is the output data. By inputting a series of teaching data into the ANN system, a simplified OBJ function at the targeted frequencies of 500 Hz, 3000 Hz, and 5000 Hz is built and described below.

7.1. Target frequency at 500 Hz

Individual design data sets are conveyed to COMSOL for acoustical simulation for the maximization of TL at 500 Hz. Subsequently, these design data sets and resulting TLs (at 500 Hz) are forwarded to the ANN for training and verification. A simplified OBJ function is then obtained and shown below:

$$\begin{aligned} &\mathrm{OBJ}_{500\mathrm{Hz}}(\mathrm{D},\mathrm{L}) \\ &= \mathrm{TL}_{500\mathrm{Hz}}(\mathrm{D},\mathrm{L}) \\ &= 315219 + 5.92244 \cdot \mathrm{NN4}_{500} \end{aligned} \tag{18a}$$

$$\mathrm{NN1}_{500} = \text{-}3.89711 + 0.0866025 \times \mathrm{D} \tag{18b}$$

$$\mathrm{NN2}_{500} = -6.49519 + 0.433013 \times \mathrm{L} \tag{18c}$$

$$\mathrm{NN4}_{500} = -0.683231\mathrm{xNN1}_{500}\text{-}0.708108\mathrm{xNN2}_{500} \tag{18d}$$

7.2. Target frequency at 3000 Hz

Similarly, for the TL maximization at 3000 Hz, the acoustical simulation of silencer's TL with respect to individual design data is also established and run on the COMSOL. These predicted TLs (at 3000 Hz)

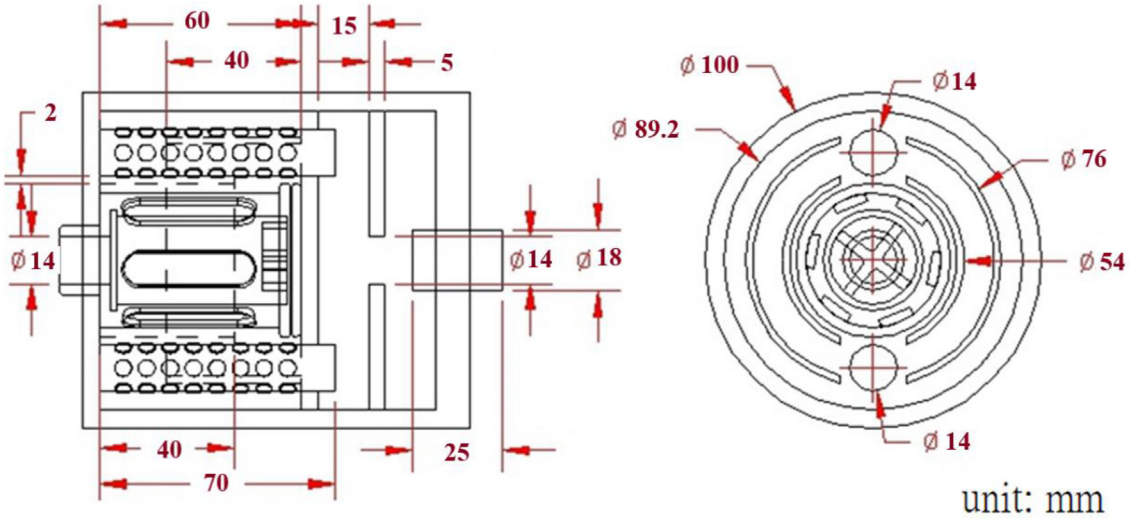

(a) Section view

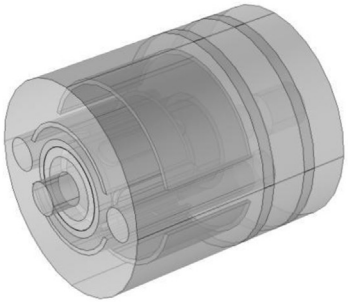

(b) 3-D view

Fig. 8. Dimension of Silencers.

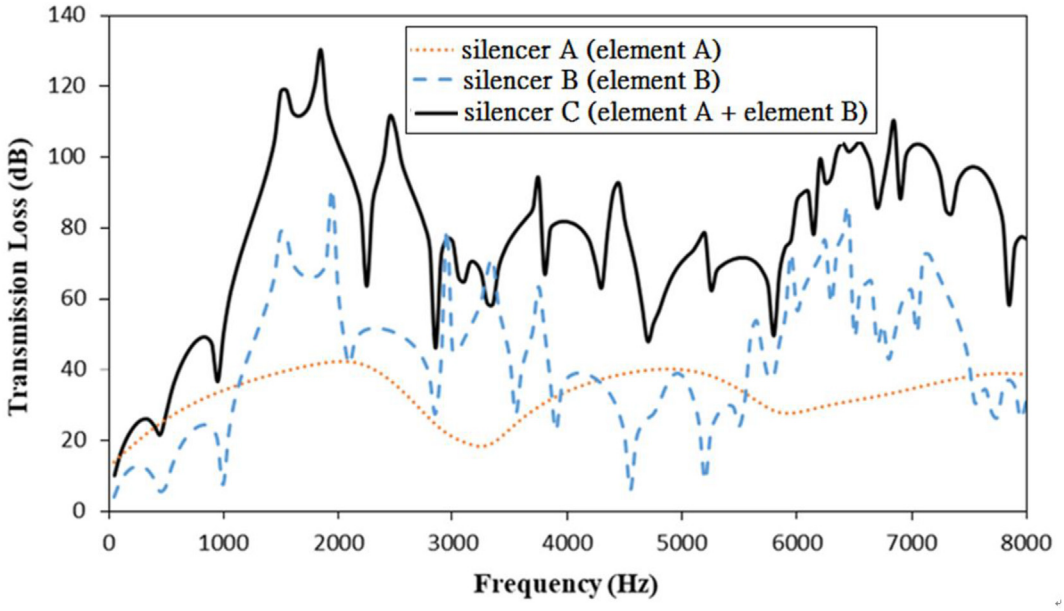

Fig. 9. Comparison of TL with respect to Silencer A~ Silencer C.

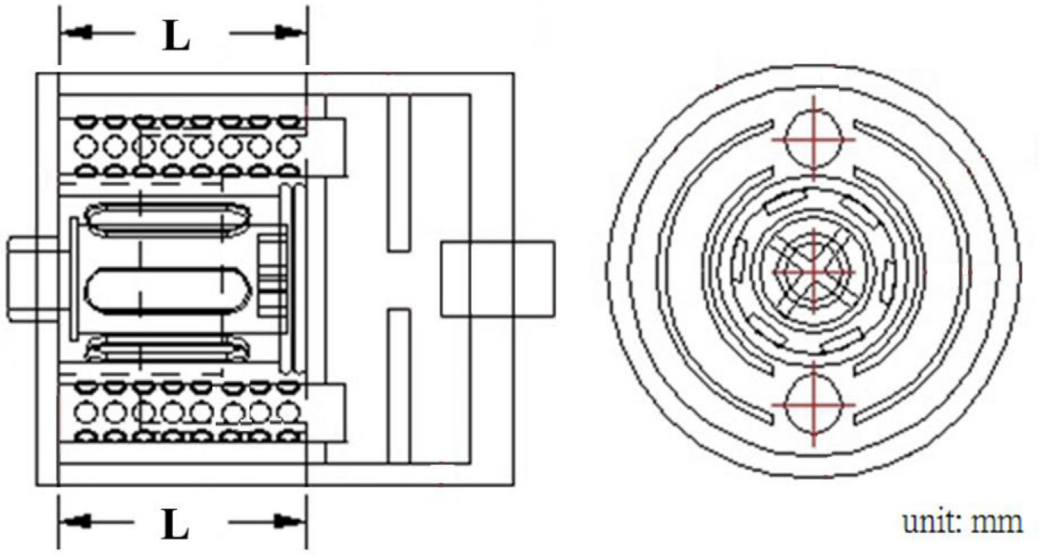

Fig. 10. Selected design parameter (L) used in sensitivity analysis.

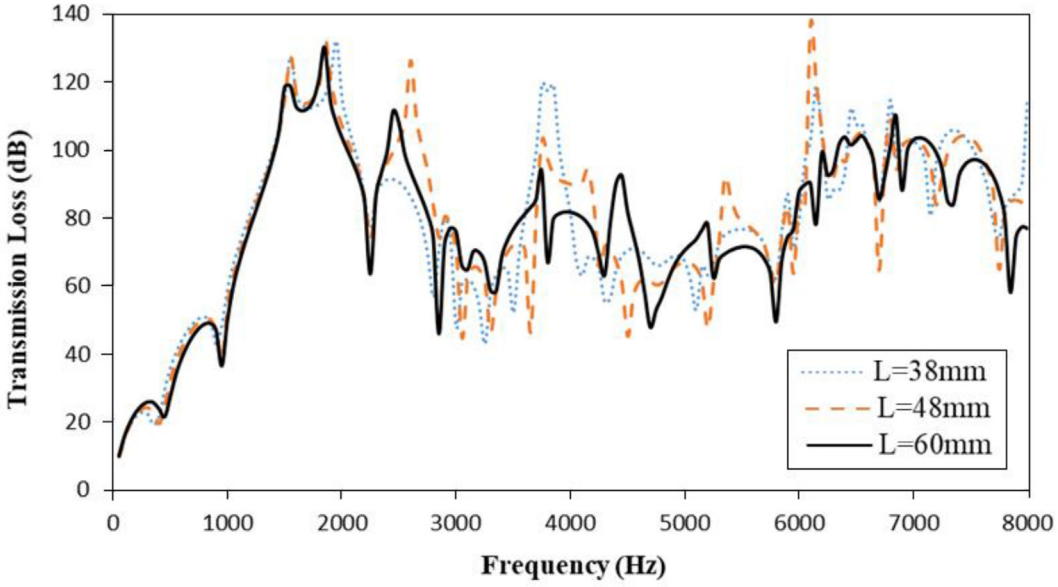

Fig. 11. Comparison of TL with respect to various value of L in Silencer C.

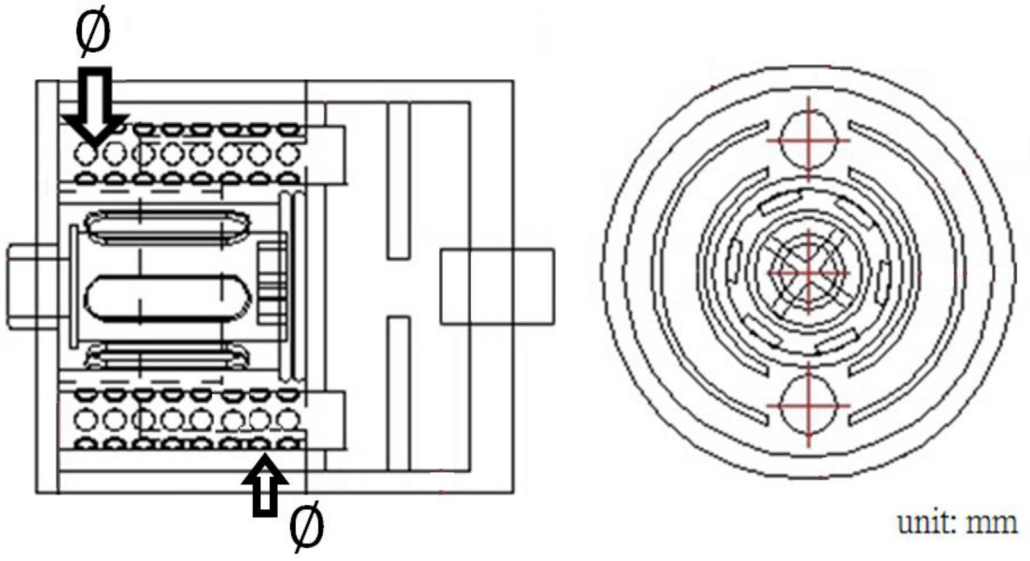

Fig. 12. Selected design parameter (∅) used in sensitivity analysis.

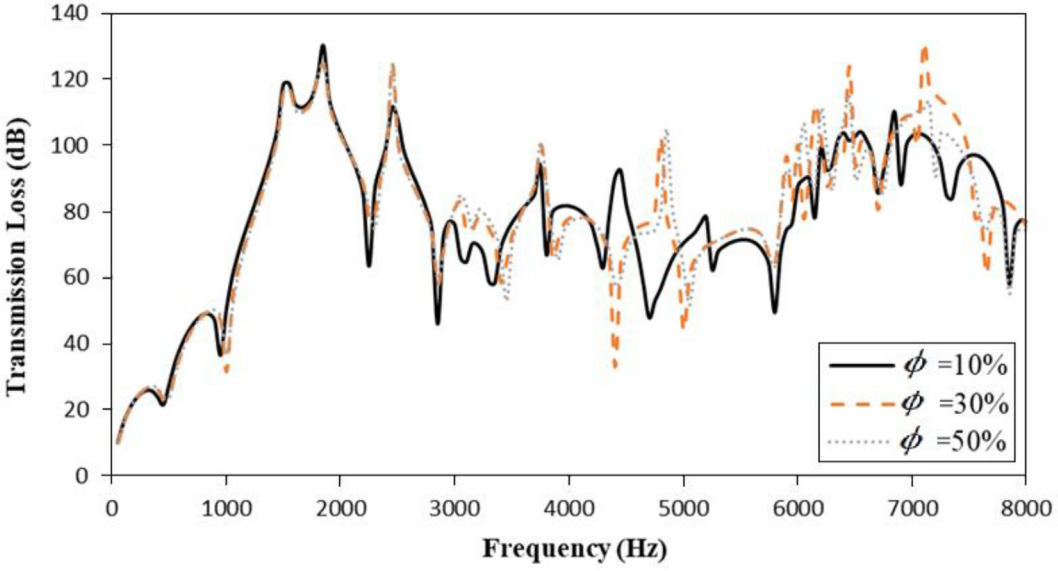

Fig. 13. Comparison of TL with respect to various value of ∅ in Silencer C.

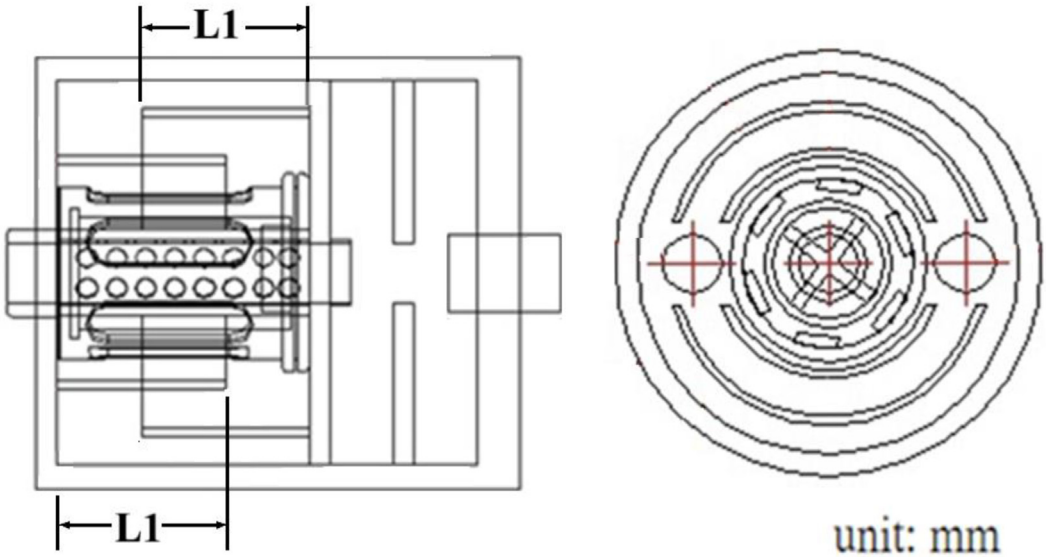

Fig. 14. Selected design parameter (L1) used in sensitivity analysis.

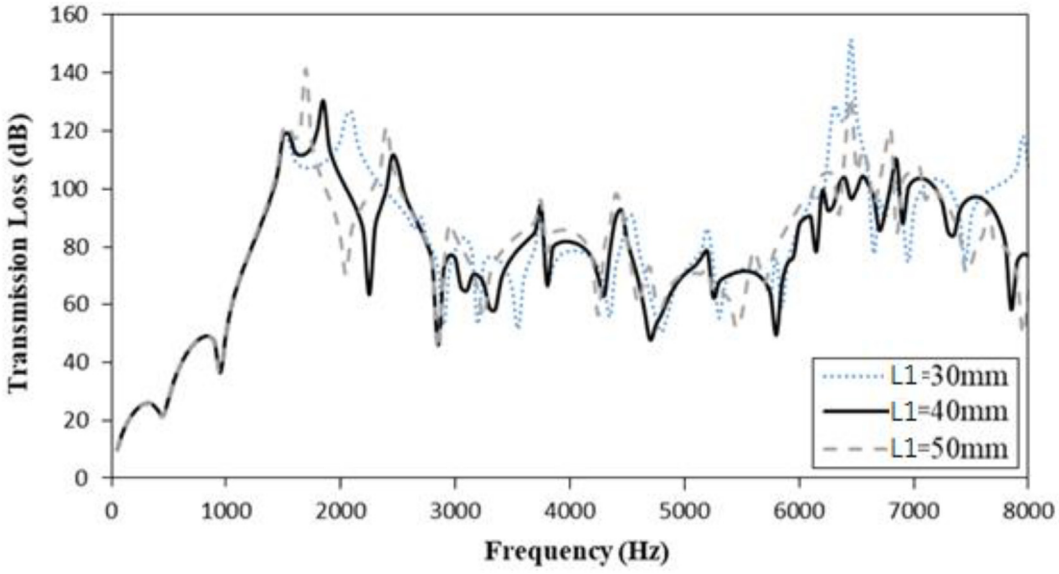

Fig. 15. Comparison of TL with respect to various value of L1 in silencer C.

together with design data sets are conveyed to the ANN for further ANN's training and confirmation. After that, a simplified OBJ function is then obtained and depicted below:

$$\mathrm{OBJ}_{3000\mathrm{Hz}}(\mathrm{D},\mathrm{L}) = \mathrm{TL}_{3000\mathrm{Hz}}(\mathrm{D},\mathrm{L}) = 66.9851 + 7.92883 \cdot \mathrm{NN4}_{3000} \quad (19a)$$

$$\mathrm{NN1}_{3000} = -3.89711 + 0.0866025 \times \mathrm{D} \quad (19b)$$

$$\mathrm{NN2}_{3000} = -6.49519 + 0.433013 \times \mathrm{L} \quad (19c)$$

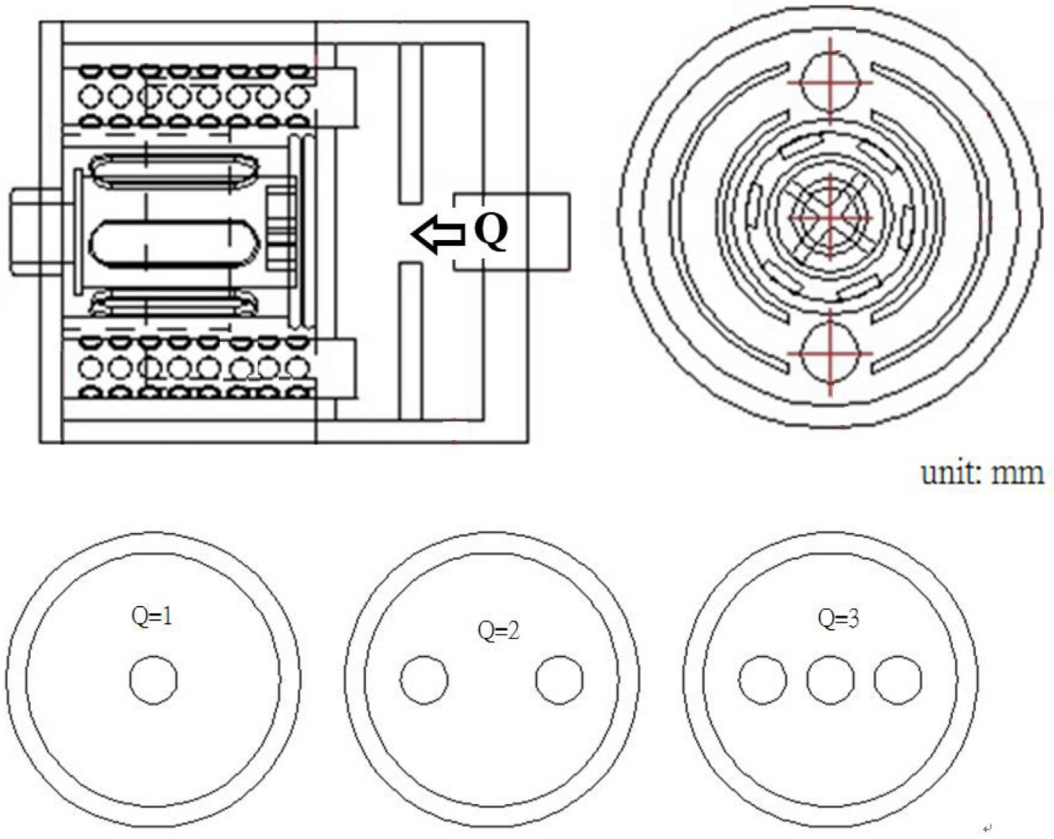

Fig. 16. Selected design parameter (Q: number of horizontal hole) used in sensitivity analysis.

$$\begin{aligned}NN4_{3000} = {} & -0.680385 + 0.605496xNN1_{3000}- \\ & 0.577622xNN2_{3000}+0.392984xNN1_{3000}^{2} \\ & +0.33276xNN2_{3000}^{2}- \\ & 0.454209xNN1_{3000}xNN2_{3000}- \\ & 0.307767xNN1_{3000}^{3}\end{aligned} \tag{19d}$$

7.3. Target frequency at 5000 Hz

Likewise, for the maximization of TL at 5000 Hz, these design data sets are adopted into COMSOL for acoustical simulation. The design data sets and resulting TLs (at 5000 Hz) are also transmitted to ANN for further ANN's training and certification. Consequently, an educated ANN serving as a simplified OBJ function is obtained and described below:

$$\begin{aligned}OBJ_{5000Hz}(D,L) & = TL_{5000Hz}(D,L) \\ & = 69.736 + 2.76929 \cdot NN5_{5000}\end{aligned} \tag{20a}$$

$$NN1_{5000} = -3.89711 + 0.0866025 \times D \tag{20b}$$

$$NN2_{5000} = -6.49519 + 0.433013 \times L \tag{20c}$$

$$\begin{aligned}NN4_{5000} = {} & -0.644395 + 0.357339xNN1_{5000}+0.84175 \\ & xNN2_{5000} +0.863732xNN1_{5000}^{2}-0.176378 \\ & xNN2_{5000}^{2}-0.396551xNN1_{5000}^{3} \\ & -0.426997xNN2_{5000}^{3}\end{aligned} \tag{20d}$$

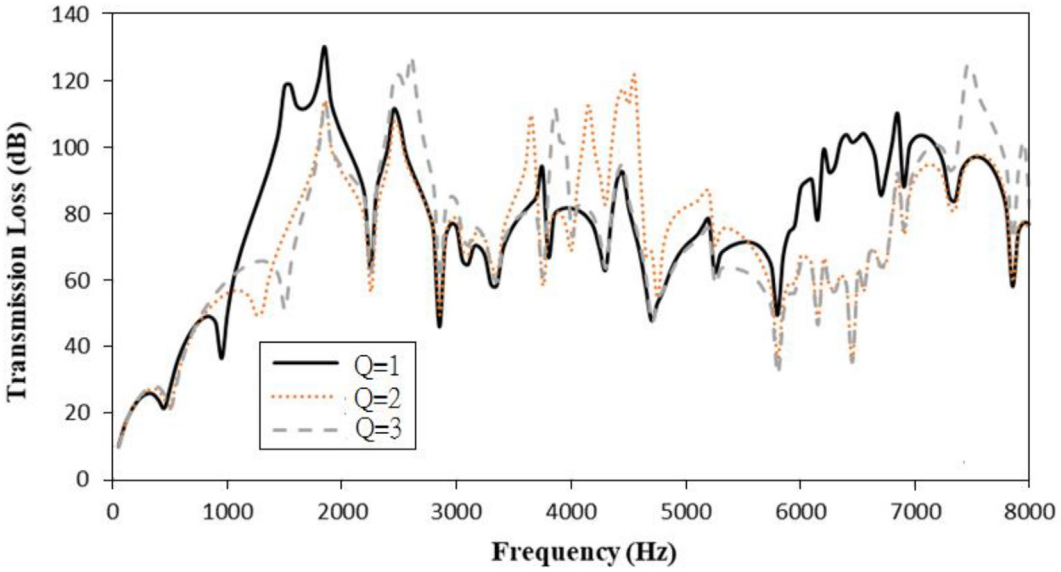

Fig. 17. Comparison of TL with respect to various value of Q in silencer C.

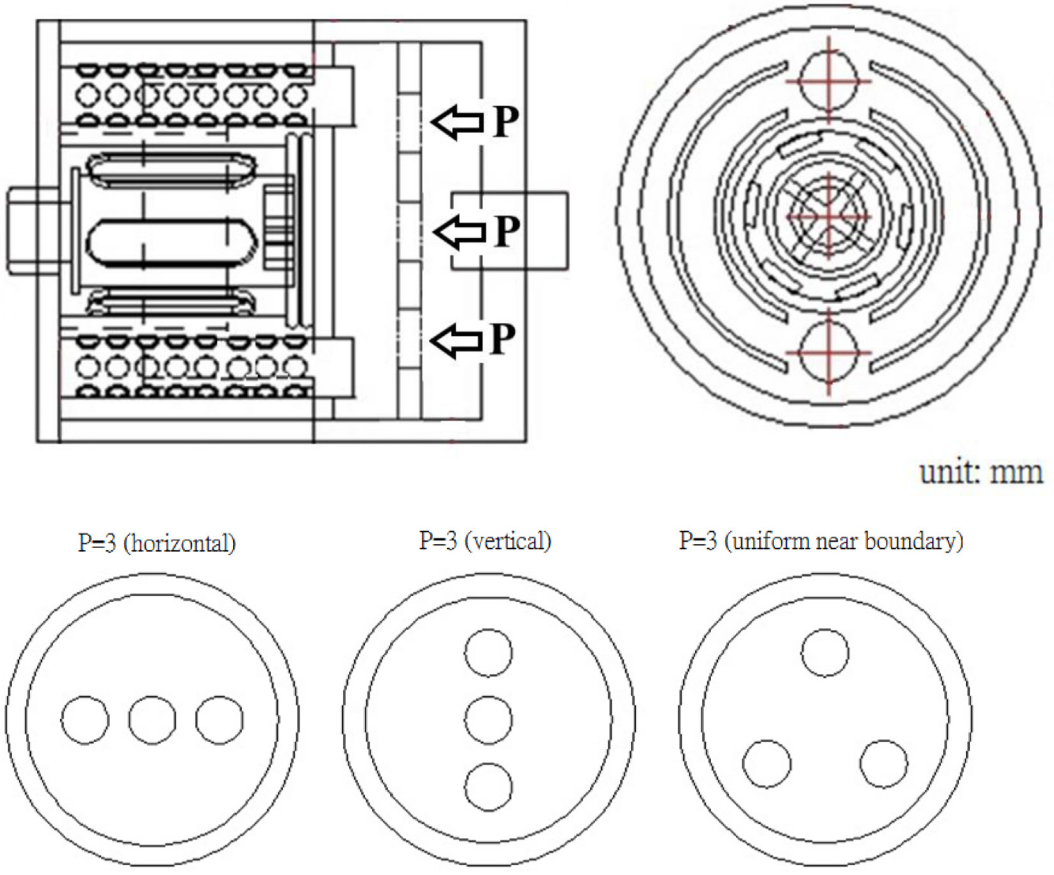

Fig. 18. Selected design parameter (hole-allocation style) used in sensitivity analysis.

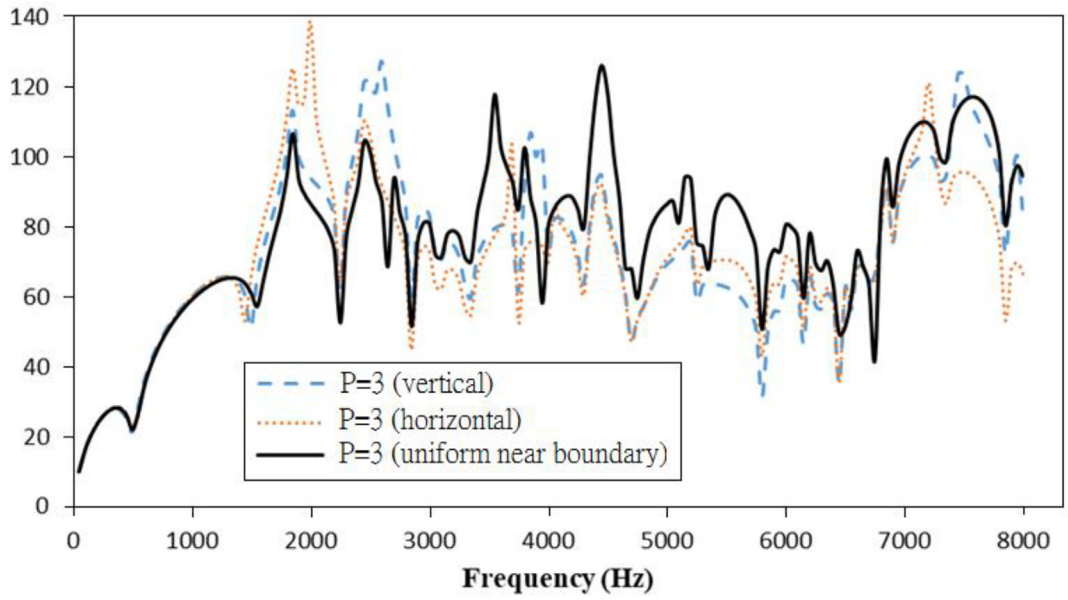

Fig. 19. Comparison of TL with respect to various allocation style of hole in silencer C.

$$NN5_{5000} = -0.370852xNN2_{5000}xNN4_{5000} + 0.816377xNN4^{3}_{5000} \quad (20e)$$

8. Results and discussion

8.1. Results

The design data of shape-optimized silencer at the specified frequencies of 500 Hz, 3000 Hz and 5000 Hz are obtained using the educated ANN and linking the ANN with GA optimizer. The GA controllers adopted in optimization process are illustrated in Table 3. As depicted in Tables 4–6, the silencer is successfully optimized at specified frequencies of 500 Hz, 3000 Hz, and 5000 Hz and compared to the original data. In addition, as illustrated in Tables 7–9, the accuracy of the ANN model is rechecked using an exact solution simulated from the COMSOL. According to Tables 7–9, the accuracies of ANN model optimized at 500 Hz, 3000 Hz, and 5000 Hz are 0.61%, 3.87%, and 7.19%, respectively.

By substituting both silencer's original design data and optimized design data into COMSOL calculation, the related TL curves before and after silencer optimization are shown in Figs. 21–23. As displayed in Fig. 23, the TLs at the specified frequency of 500 Hz before and after silencer optimization are 26.3 dB and 41.9 dB. Additionally, as plotted in Fig. 22, the TLs at the specified frequency of 3000 Hz before and after silencer optimization are 75.3 dB and 80.6 dB. Finally, as demonstrated in Fig. 23, the TLs at the specified frequency of 5000 Hz before and after the silencer optimization are 70.3 dB and 83.4 dB, respectively.

8.2. Discussion

As described in section 6, the influence of TL respecting the geometry of a perforated tube is obvious. As shown in Fig. 11, in the L = 48 case, TL spectrum is horizontally shifted to the right when the frequency is below 3000 Hz; in the case of L = 38, TL spectrum is horizontally shifted to the right when the frequency is below 2000 Hz; and, as indicated in Fig. 13, the TL spectrum after 2800 Hz fluctuates visibly when ∅ increases. In addition, Fig. 14 reveals that the TL after 1500 Hz is horizontally shifted to the right when varying the L1. Also, Fig. 17 indicates that the impact of TL related to Q (the number of horizontal holes on the orifice plate) after 800 Hz is apparent. For the frequency range between 800 Hz and 2500 Hz, the TL rises as

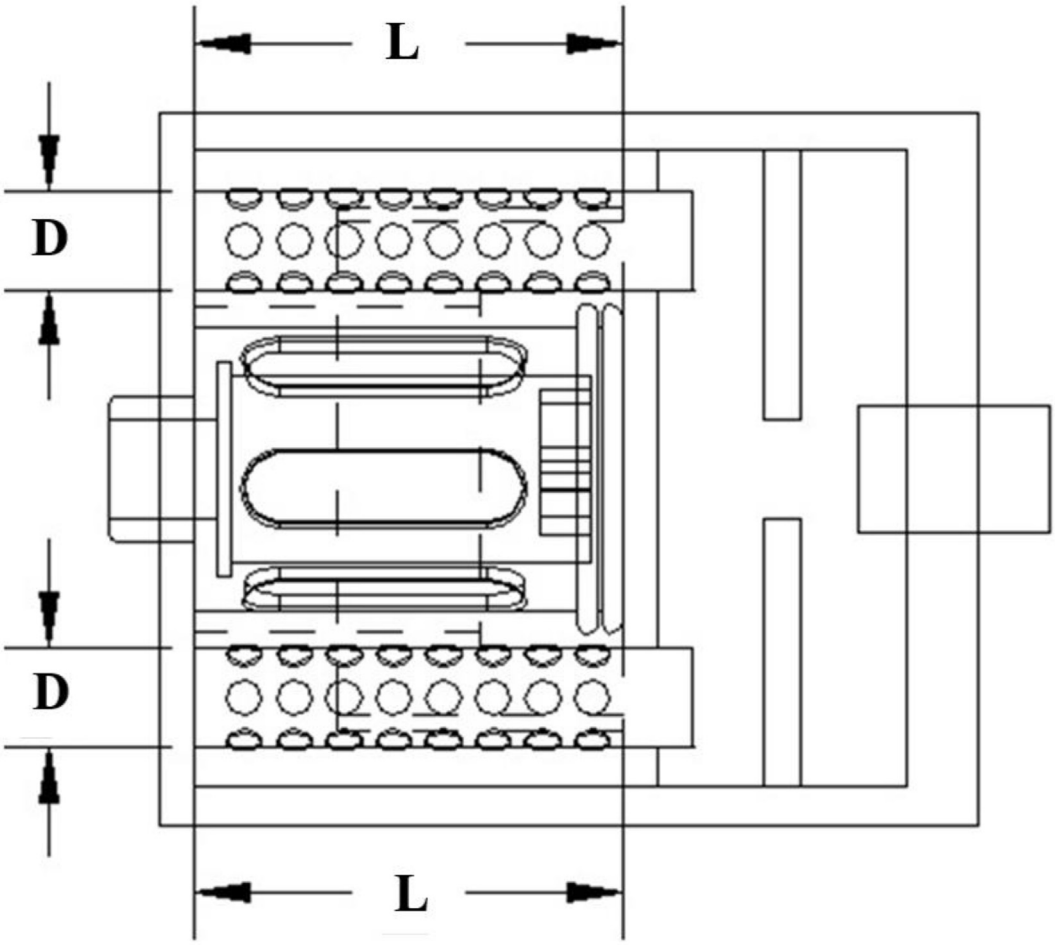

(a) 2-D drawing

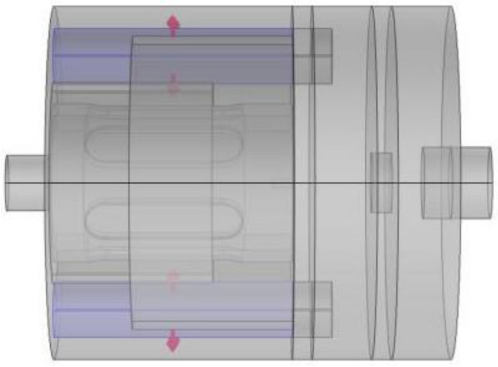

(b) 3-D drawing

Fig. 20. Selected design parameters of D and L used in shape optimization.

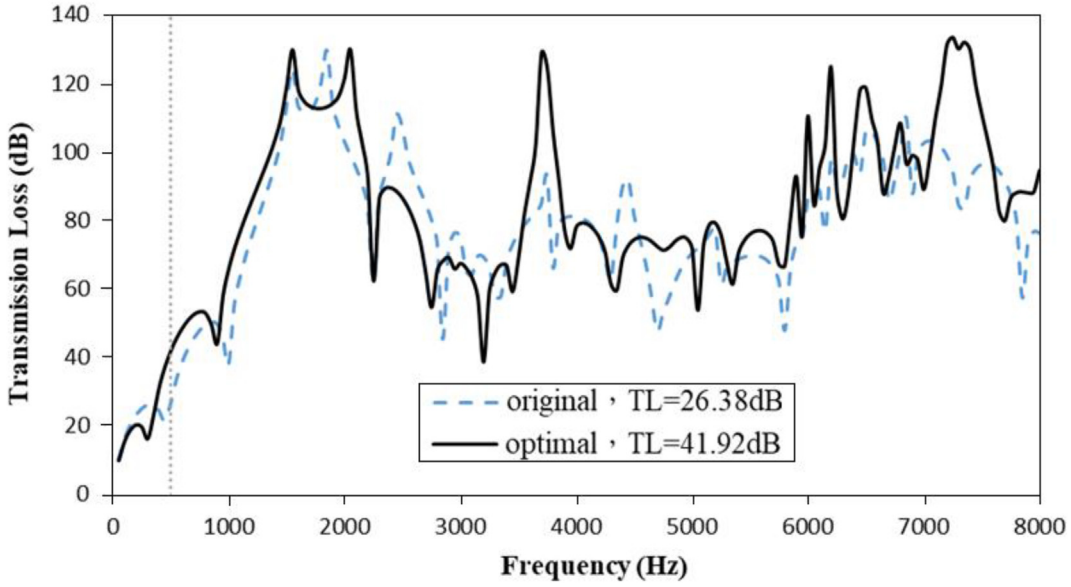

Fig. 21. Comparison of TL before and after optimization of silencer C is performed (target frequency of 500 Hz).

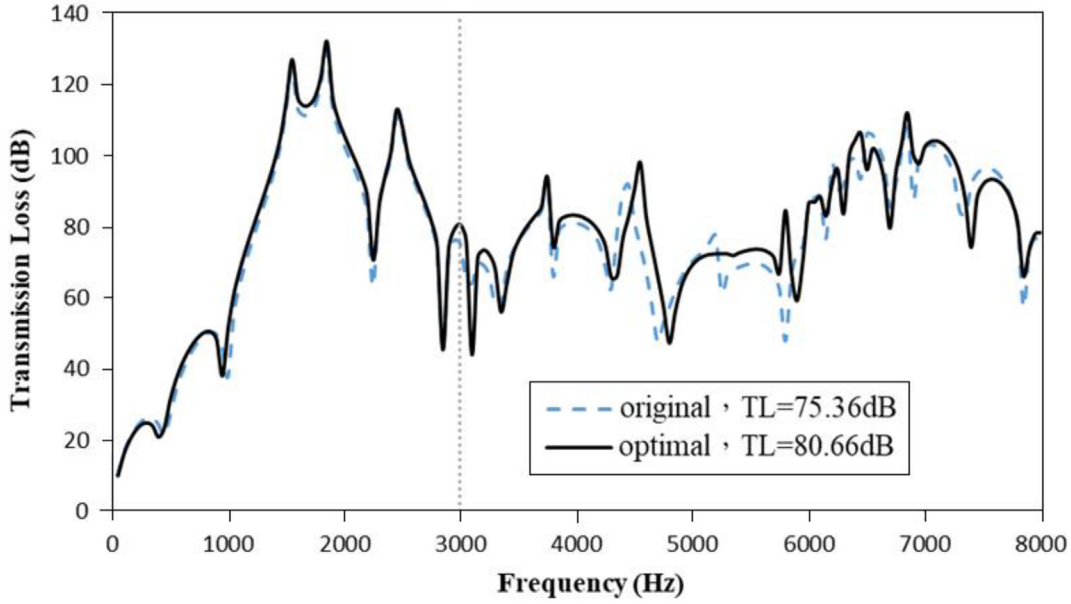

Fig. 22. Comparison of TL before and after optimization of silencer C is performed (target frequency of 3000 Hz).

Q declines. Moreover, the influence of TL respecting the hole-allocation pattern in an orifice plate (with three holes) is also remarkable. Result in Fig. 19 indicates that the fluctuation of TL after 1250 Hz is noticeable when the hole-allocation pattern changes.

For the silencer C's optimization, the numerical results using the parameter set D and L are shown

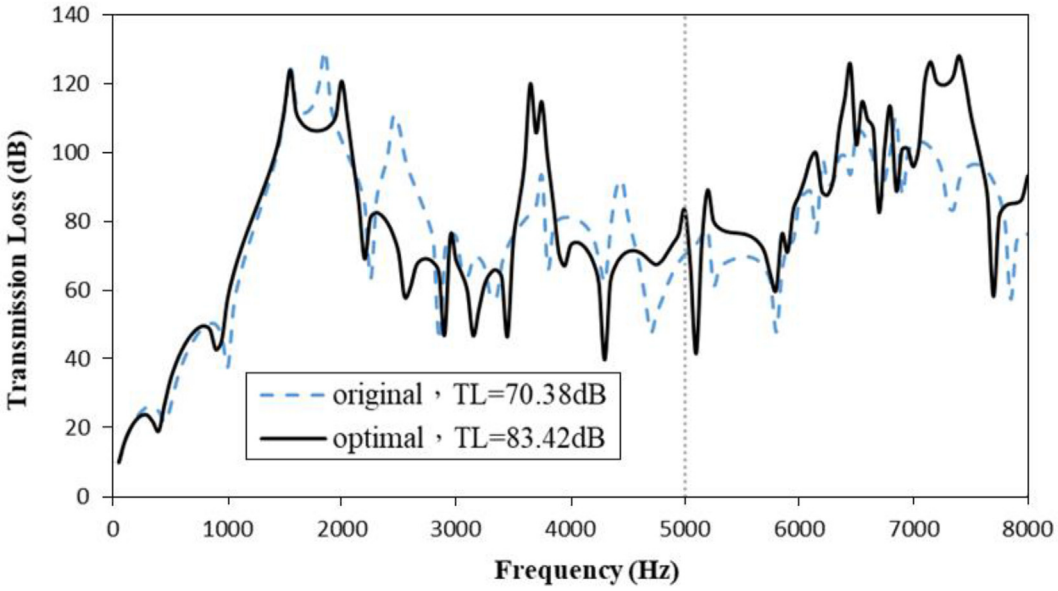

Fig. 23. Comparison of TL before and after optimization of silencer C is performed (target frequency of 5000 Hz).

Table 1. The relationship between the diameter (D) and the (L) of perforated tube in silencer C

parameter	Min (mm)	Max (mm)	4 Level (mm)			
D (mm)	12	18	12	14	16	18
L (mm)	30	60	30	40	50	60

Table 2. The selected level and related parameter set

NO. of Exp.	*D* (mm)	*L* (mm)
1	12	30
2	12	40
3	12	50
4	12	60
5	14	30
6	14	40
7	14	50
8	14	60
9	16	30
10	16	40
11	16	50
12	16	60
13	18	30
14	18	40
15	18	50
16	18	60

in Tables 4−9 and Figs. 21−23. The noise abatement of muffler C at these specified tones of 500 Hz, 3000 Hz, and 5000 Hz is enhanced by 15.6 dB, 5.3 dB, and 13.1 dB, respectively. Furthermore, as designated in Tables 7−9, a correctness check of the ANN models at 500 Hz, 3000 Hz, and 5000 Hz by the FEM calculation falls between 0.61% and 7.19%. Therefore, the simplified OBJ using ANN model is applicable and adopted in further GA optimization.

Table 3. The genetic algorithm's controllers set using in the GA optimization process

GA controllers	Value or strategy
Population	generated random
crossover	uniform crossover
elitism	open
Selection strategy	Elitism
$iter_m$	1000
Bit_n	20
pop_n	100
pc_n	0.6
pm_n	0.5

Table 4. The comparison of related design parameters before and after optimization at 500 Hz is performed

Design parameter (mm)	*D*	*L*
Before optimization	14	60
After optimization (at 500 Hz)	12.01	30.11

Table 5. The comparison of related design parameters before and after optimization at 3000 Hz is performed

Design parameter (mm)	*D*	*L*
Before optimization	14	60
After optimization (at 3000 Hz)	12.03	59.83

Table 6. The comparison of related design parameters before and after optimization at 5000 Hz is performed

Design parameter (mm)	*D*	*L*
Before optimization	14	60
After optimization (at 5000 Hz)	16.56	30.01

Table 7. Accuracy check between the ANN model and COMSOL (optimal design set at 500 Hz)

	TL (dB)	Error (%)
TL (optimal design parameter set at 500 Hz) obtained by ANN in conjunction with GA	42.18	**0.61**
TL (optimal design parameter set at 500 Hz) calculated by COMSOL	41.92	

Table 8. Accuracy check between the ANN model and COMSOL (optimal design set at 3000 Hz)

	TL (dB)	error (%)
TL (optimal design parameter set at 3000 Hz) obtained by ANN in conjunction with GA	83.91	**3.87**
TL (optimal design parameter set at 3000 Hz) calculated by COMSOL	80.66	

Table 9. Accuracy check between the ANN model and COMSOL (optimal design set at 5000 Hz)

	TL (dB)	error (%)
TL (optimal design parameter set at 5000 Hz) obtained by ANN in conjunction with GA	77.42	**7.19**
TL (optimal design parameter set at 5000 Hz) calculated by COMSOL	83.42	

9. Conclusions

The noise level emitted from pneumatic venting equipment is huge due to high pressure and venting velocity. Traditional noise abatement using a porous plug made of resin is found to be inefficient. So as to efficiently reduce the noise emitted from a pneumatic equipment, three silencer designs using element A (a penetrable resin plug only), element B (a shell composing of extended tubes, two perforated tubes, and an orifice plate), and hybrid unit (element A + element B) are explored. Simulation results reveal that the silencer composing of element A and element B is superior to others. Therefore, silencer C is chosen as the acoustical mechanism. Moreover, sensitivity analysis of silencer C demonstrates that the perforated tube's geometric parameters have significant acoustical influence. Hence, both the diameter (D) and horizontal length (L) of the perforated tube are chosen as the design parameters during the silencer optimization. As silencer C features complicated mechanism, a neural network (ANN) used to serve as a simplified OBJ function is established to ease the simulation and shorten the optimization process by teaching and testing the ANN system with data sets (input data of silencer's dimension and output data of TL simulated by COMSOL). With the ANN model fully educated and tested, the optimization process is carried out by using the ANN (a simplified OBJ function) together with the GA optimizer. The results reveal that the TLs at the specified tones of 500 Hz, 3000 Hz, and 5000 Hz is enhanced by 15.6 dB, 5.3 dB, and 13.1 dB.

References

[1] Delany ME, Bazley EN. Acoustical properties of fibrous absorbent materials. Appl Acoust 1970;3(2):105−16.

[2] Johnson DL, Koplik J, Dashen R. Theory of dynamic permeability and tortuosity in fluid-saturated porous media. J Fluid Mech 1987;176:379−402.

[3] Champoux Y, Allard JF. Dynamic tortuosity and bulk modulus in air-saturated porous media. J Appl Phys 1991; 70(4):1975−9.

[4] Lafarge, Denis, et al. Dynamic compressibility of air in porous structures at audible frequencies. J Acoust Soc Am 1997;102(4):1995−2006.

[5] Cummings A. Sound transmission in curved ducts bends. J Sound Vib 1974;35:451−77.

[6] Rostafinski W. Transmission of wave energy in curved ducts. J Acoust Soc Am 1974;56:1005−7.

[7] Fuller CR, Bies DA. Propagation of sound in a curved bend containing curved axial partition. J Acoust Soc Am 1978;63: 681−6.

[8] Selamet A, Dickey NS, Novak JM. The theory of hershel-quinckee tube: a theoretical computational and experimental investigation. J Acoust Soc Am 1994;96:3177−85.

[9] Kim JT, Ih JG. Transfer matrix of curved duct bends and sound attenuation in curved expansion chambers. Appl Acoust 1999;56:297−309.

[10] Yeh LJ, Chang YC, Chiu MC. Numerical studies on constrained venting system with reactive mufflers by GA optimization. Int J Numer Methods Eng 2006;65:1165−85.

[11] Bogdanowicz A, Kniaziewicz T. Marine diesel engine exhaust emissions measured in ship's dynamic operating conditions. Sensors 2020;20(6589):1−21.

[12] Shaw J, Wang YH, Lin CY. Sound and vibration analysis of a marine diesel engine via reverse engineering. J Mar Sci Technol 2018;26(5):703−11.

[13] Lee TK, Joo WH, Bae JG. Exhaust noise control of marine diesel engine using hybrid silencer. Trans Kor Soc Noise Vibr Eng 2009;19(7):679−84.

[14] Sunarsih S, Nugroho TF, Navyazka MY. Noise reduction in ship engine room by optimisation of muffler design. Int J Mar Eng Innov Res 2020;5(4):224−33.

[15] Dhaiban AA, Soliman MS, El-Sebaie MG. Finite element simulation of acoustic attenuation performance of elliptical muffler chambers. J Eng Sci 2011;39(6):1361−73.

[16] Fu J, Xu M, Zhang Z, Kang W, He Y. Muffler structure improvement based on acoustic finite element analysis. J Low Freq Noise Vib Act Control 2019;38(2):415−26.

[17] Lin TW, Hsieh JC, Chindakham N, Hai PD. Optimal design of the composite laminate hydrogen storage vessel. J Energy Res 2013;37:761−8.

[18] Chang YC, Chiu MC, Cheng MM. Optimum design of perforated plug mufflers using neural network and genetic algorithm. Proc ImechE Part C: J Mech Eng Sci 2009;223: 935−52.

[19] Hwang PU. *A study on the straight-through mufflers*, Master degree. Taipei, Taiwan: Taiwan University; 2001.

[20] Jeon S, Kim D, Hong C, Jeong W. Acoustic performance of industrial mufflers with CAE modeling and simulation. Int J Nav Archit Ocean Eng 2014;6(4):935−46.

[21] Barbosa LR, Lenzi A. Parametric optimization and analysis of metallic porous material used for discharge system of hermetic compressor. Appl Acoust 2018;136:94−101.

[22] Ivakhnenko, Grigorevich A. Polynomial theory of complex systems. IEEE Trans Syst Man Cybern 1971;4: 364−78.

[23] Amiri1 M, Soleimani S. ML-based group method of data handling: an improvement on the conventional GMDH. Compl Intell Syst 2021;7:2949−60.

[24] Chang YC, Yeh LJ, Chiu MC, Lai GJ. Shape optimization on constrained single-layer sound absorber by using GA method and mathematical gradient methods. J Sound Vib 2005;286(4−5):941−61. 2005.

[25] Chang YC, Yeh LJ, Chiu MC. Shape optimization on constrained single-chamber muffler by using GA method and mathematical gradient method. Int J Acoust Vib 2005;10(1): 17−25.

[26] Chiu MC, Chang YC, Yeh LJ, Lai GJ, Her MG, Tu CC, Lan TS, Cheng HC. Shape optimization of double-chamber mufflers with extended tube and side inlet/outlet by using four-pole transfer matrix method, boundary element method and genetic algorithm. J Chin Soc Mech Eng 2006;27(6): 825−32.

[27] Holland J. Adaptation in natural and artificial system. Ann Arbor: University of Michigan Press; 1975.

[28] Jong D. An analysis of the behavior of a class of genetic adaptive systems. Doctoral thesis. Dept Computer and Communication Sciences, Ann Arbor, University of Michigan; Ann Arbor, Michigan State, USA; 1975.